

Carbon Monoxide Clouds at Low-Metallicity in the WLM Galaxy

Bruce G. Elmegreen¹, Monica Rubio², Deidre A. Hunter³, Celia Verdugo², Elias Brinks⁴, & Andreas Schruba⁵

¹*IBM Research Division, T.J. Watson Research Center, 1101 Kitchawan Road, Yorktown Heights, NY 10598, USA*

²*Departamento de Astronomía, Universidad de Chile, Casilla 36-D, Santiago, Chile*

³*Lowell Observatory, 1400 West Mars Hill Road, Flagstaff, Arizona 86001 USA*

⁴*Centre for Astrophysics Research, University of Hertfordshire, Hatfield AL10 9AB, UK*

⁵*Cahill Center for Astronomy and Astrophysics, California Institute of Technology, Pasadena, CA 91125, USA*

Carbon monoxide (CO) is the primary tracer for interstellar clouds where stars form, yet CO has never been detected in galaxies with an oxygen abundance relative to hydrogen less than 20% of solar, even though such low metallicity galaxies often form stars. This raises the question of whether stars can form in dense gas without the usual molecules, cooling to the required near-zero temperatures by atomic transitions and dust radiation rather than molecular line emission¹, and it highlights uncertainties about star formation in the early universe, when the metallicity was generally low. Here we report the detection of CO in two regions of a local dwarf irregular galaxy, WLM, where the metallicity is 13% of the solar value^{2,3}. New sub-millimeter observations and archival far-infrared observations are used

to estimate the cloud masses, which are both slightly larger than $10^5 M_{\odot}$. The clouds have produced stars at a rate per molecule equal to 10% of that in the local Orion Nebula cloud. The CO fraction of the molecular gas is also low, about 3% of the Milky Way value. These results suggest that both star-forming cores and CO molecules become increasingly rare in H_2 clouds as the metallicity decreases in small galaxies.

Wolf-Lundmark-Melotte (WLM) is an isolated dwarf galaxy at the edge of the Local Group⁴. It has a low star formation rate because of its small size, and like other dwarf Irregulars (dIrr), no previous evidence⁵ for the molecular gas that always accompanies young stars in larger galaxies⁶. One problem is that the dominant tracer of such gas is carbon monoxide (CO), and dIrr galaxies have low carbon and oxygen abundances relative to hydrogen. No galaxy with O/H abundance less than 20% has been detected in CO⁷⁻⁹. Far more abundant is H_2 , but this does not have an observable state of excitation at the low temperatures ($\sim 10 - 30$ K) required for star formation.

To search for star-forming gas, we surveyed WLM for CO($J = 3 - 2$) and continuum dust emission at 345 GHz using the Atacama Pathfinder EXperiment (APEX) telescope at Llano de Chajnantor, Chile, with the the Swedish Heterodyne Facility Instrument (SHFI¹⁰) and the Large APEX Bolometer Camera (LABOCA¹¹). We also used a map of dust emission at $160 \mu\text{m}$ from the *Spitzer* Local Volume Legacy Survey¹², and a map of atomic hydrogen re-reduced from the archives of the Jansky Very Large Array radio telescope. The dust measurements convert to a dust temperature and dust mass, and after applying a suitable gas-to-dust ratio, convert to a gas mass from which the HI mass can be subtracted to give the H_2 mass for comparison to CO.

Figure 1 shows WLM and the two regions where we detected CO(3-2) emission, along with HI, far-infrared and sub-mm images. Observed and derived parameters are in Tables 1 and 2, respectively. The peak CO brightness temperature in each detected region is $\sim 0.01 - 0.015$ K and the FWHM linewidth is ~ 12 km s⁻¹. Previous efforts to detect CO(1-0) in WLM⁵ partially overlapped Region A with a 45'' aperture and concluded a 5σ upper limit to the CO(1-0) intensity of 0.18 K km s⁻¹. Our observation with an 18'' aperture measures 0.200 ± 0.046 K km s⁻¹ for CO(3-2) in the same region. The difference arises because the CO cloud is unresolved even by our 18'' beam – we did not detect comparable CO(3-2) intensities in our searches adjacent to Region A. The previous upper limit corresponds to a maximum CO(1-0) luminosity of 8300 K km s⁻¹ pc² inside 45'' (which is 215 pc at WLM), whereas the cloud we detect has a CO(3-2) luminosity ~ 6 times smaller, 1500 K km s⁻¹ pc². Likewise, the previous null detection⁵ in CO(2-1) claimed a 5σ upper limit that is about the same as our CO(3-2) detection, but their closest pointing differed from our Region A by ~ 70 pc (14'' or half the beam diameter at CO(2-1)), which could have been enough to take it off the cloud.

The 160 μ m, 870 μ m and HI peaks are slightly offset from the CO positions, indicating variations in temperature and molecular fraction. A large HI and FIR cloud that surrounds Region A, designated A1, was used to measure dust temperature, $T_d \sim 15$ K, which was assumed to apply throughout the region (the 160 μ m observation does not resolve Region A so a more localized temperature measurement is not possible). T_d was determined from the 870 μ m and 160 μ m fluxes corrected for the CO(3-2) line and broadband free-free emission (Table 1) assuming a modified black body function with dust emissivity proportional to the power β of frequency. Local

measurements¹³ suggest $\beta = 1.78 \pm 0.08$, although a range is possible^{14,15}, depending on grain temperature and properties¹⁶. The 870 μm flux was also corrected for an unexplained FIR and sub-mm excess that is commonly observed in other low metallicity galaxies^{17,18}. An alternate combination of lower β with no sub-mm correction¹⁹ gives similar results (suppl. material). The dust mass was calculated from an emissivity¹⁴ of $\kappa = 13.9 \text{ cm}^2 \text{ gm}^{-1}$ at 140 μm , and converted to 870 μm with the same power law index β . The dust mass for Region A is then $M_{dust,A} = S_{870,A} D^2 / \kappa B_\nu(T_d)$ for flux $S_{870,A}$, distance D , and Black-Body function B_ν .

Dust mass is converted to gas mass with a factor equal to the gas-to-dust mass ratio, R_{GD} . An approximation⁸ is to assume the solar value²⁰ ($1/0.007$) increased by the inverse of the metallicity of WLM (0.13), which would give 1100. We use this approximation here, but allow for a scaling factor to the gas mass, $\delta_{GD} = R_{GD}/1100$; i.e., the gas-to-dust ratio normalized to the Milky Way and scaled to the metallicity.

The results are in Table 2 assuming $\beta = 1.8$ as the fiducial value, and also $\beta = 1.6$ and 2 to illustrate the dependence of the results on β . Dust and gas mass correlate¹⁵ with the assumed β . The total gas mass column density in a 22'' region around position A is $\sim 58 \pm 15 M_\odot \text{ pc}^{-2}$ for $\beta = 1.8$. Atomic hydrogen contributes $\sim 27.3 \pm 1.4 M_\odot \text{ pc}^{-2}$, and the remainder is ascribed to molecular H_2 traced by the observed CO.

The integral under the CO(3-2) line from Cloud A is $I_{CO} = 0.200 \pm 0.046 \text{ K km s}^{-1}$. This has to be converted to CO(1-0) before comparing it with H_2 mass in the conventional way. We take as a guide²¹ the CO(3-2)/CO(1-0) ~ 0.80 ratio in another low metallicity galaxy, the Small Magel-

lanic Cloud²² (SMC, where $O/H = 20\%$). The result, 0.25 K km s^{-1} , is combined with the H_2 mass column density to determine the conversion factor, α_{CO} , from $\text{CO}(1-0)$ to H_2 . If α_{CO} can be calibrated as a function of metallicity, then CO observations can be used directly to infer the molecular gas content irrespective of the dust spectral energy distribution. Extensive compilations⁷⁻⁹ show α_{CO} increasing strongly at lower metallicity, from $\sim 4 M_{\odot} \text{ pc}^{-2} (\text{K km s}^{-1})^{-1}$ in the Milky Way⁸ where the metallicity³ is $12 + \log(O/H) = 8.69$, down to the previous CO detection limit⁸ in the SMC where $\alpha_{\text{CO}} \sim 70 M_{\odot} \text{ pc}^{-2} (\text{K km s}^{-1})^{-1}$ at $12 + \log(O/H) = 8.0$. Our observations of WLM² at $12 + \log(O/H) = 7.8$ continue this trend.

Taking the H_2 column density from the residual between the dust-derived total and the HI column density, $31 \pm 15 M_{\odot} \text{ pc}^{-2}$, and dividing by the inferred $\text{CO}(1-0)$ line integral of 0.25 K km s^{-1} , we obtain $\alpha_{\text{CO}} = 124 \pm 60 M_{\odot} \text{ pc}^{-2} (\text{K km s}^{-1})^{-1}$ including Helium and heavy elements, with a range in α_{CO} from 34 to 271 as β varies from 1.6 to 2. The corresponding X_{CO} factor for H_2 column density conversion from I_{CO} would be $(5.8 \pm 2.8) \times 10^{21} \text{ cm}^{-2} (\text{K km s}^{-1})^{-1}$, with a range from 1.5×10^{21} to 1.3×10^{22} with β . There is a large uncertainty because of the unknown dust properties (β , κ , δ_{GD} , sub-mm excess) and molecular excitation ($\text{CO}(3-2)/\text{CO}(1-0)$) in dIrr galaxies.

The star formation rate based on the $\text{H}\alpha$ and FUV²³ fluxes within an $18''$ diameter aperture centered on Cloud A is $3.9 - 4.8 \times 10^{-5} M_{\odot} \text{ yr}^{-1}$. Dividing these rates into the CO-associated molecular mass with $\alpha = 124 M_{\odot} \text{ pc}^{-2} (\text{K km s}^{-1})^{-1}$ gives a CO-molecular consumption time of 4.6-3.8 Gyr for region A. In Region B, the star formation rates by these two tracers are 1.7 -

$12.6 \times 10^{-5} M_{\odot} \text{ yr}^{-1}$ and the CO-molecular consumption time is 6.7-1.5 Gyr. These times are only slightly larger than the average value in spiral galaxies²⁴, which is ~ 2 Gyr, but they are $10\times$ larger than the rate per molecule in local giant molecular clouds²⁵, which is a more direct analogy with our observations.

The detection of CO in WLM suggests that star formation continues to occur in dense molecular gas even at lower metallicities than previously observed. The similarity between the metallicities of dIrr galaxies like WLM and those of larger galaxies at high redshift²⁶ implies that we should be able to study star formation in young galaxies using the usual techniques.

1. Krumholz, M.R. “Star Formation in Atomic Gas.” *Astrophys. J.*, **759**, 9, 9
2. Lee, H., Skillman, E. D., & Venn, K. A. “Investigating the possible anomaly between nebular and stellar oxygen abundances in the dwarf irregular galaxy WLM.” *Astrophys. J.*, **620**, 223–237 (2005)
3. Asplund, M., Grevesse, N., Sauval, A.J., & Scott, P. “The chemical composition of the sun.” *Ann. Rev. Astron. Astrophys.*, **47**, 481–522 (2009)
4. Leaman, R., et al. “The resolved structure and dynamics of an isolated dwarf galaxy: a VLT and Keck spectroscopic survey of WLM2012.” *Astrophys. J.*, **750**, 33, 20 (2012)
5. Taylor, C. L., & Klein, U. 2001, “A search for CO in the Local Group dwarf irregular galaxy WLM.” *Astron. Astrophys.*, **366**, 811–816 (2001)

6. Bigiel, F., et al. “A Constant Molecular Gas Depletion Time in Nearby Disk Galaxies.” *Astrophys. J.*, **730**, L13, 6
7. Taylor, C. L., Kobulnicky, H. A., & Skillman, E. D. “CO Emission in Low-Luminosity, H I-rich Galaxies.” *Astron. J.*, **116**, 2746–2756 (1998)
8. Leroy, A.K. et al. “The CO-to-H₂ conversion factor from infrared dust emission across the Local Group.” *Astrophys. J.*, **737**, 12, 13 (2011)
9. Schruba, A. et al. “Low CO luminosities in dwarf galaxies.” *Astron. J.*, **143**, 138, 18 (2012)
10. Vassilev, V. et al. “A Swedish heterodyne facility instrument for the APEX telescope.” *Astron. Astrophys.*, **490**, 1157-1163 (2008)
11. Siringo, G. et al., “The Large APEX BOlometer CAmera LABOCA.” *Astron. Astrophys.*, **497**, 945–962 (2009)
12. Dale, D.A. et al., “The Spitzer Local Volume Legacy: survey description and infrared photometry.” *Astrophys. J.*, **703**, 517–556 (2009)
13. Planck Collaboration et al. “Planck early results. XXV. Thermal dust in nearby molecular clouds.” *Astron. Astrophys.*, **536**, A25, 18 (2011)
14. Draine, B.T. “Interstellar dust grains.” *Ann. Rev. Astron. Astrophys.*, **41**, 241–289 (2003)
15. Galametz, M. et al. “Mapping the cold dust temperatures and masses of nearby KINGFISH galaxies with Herschel.” *Mon. Not. R. Astron. Soc.*, **425**, 763–787 (2012)

16. Coupeaud et al. “Low-temperature FIR and submillimetre mass absorption coefficient of interstellar silicate dust analogues.” *Astron. Astrophys.*, **535**, A124, 15 (2011)
17. Galametz, M. et al. “Probing the dust properties of galaxies up to submillimetre wavelengths. II. Dust-to-gas mass ratio trends with metallicity and the submm excess in dwarf galaxies.” *Astron. Astrophys.*, **532**, A56, 18 (2011)
18. Verdugo, C. “Sub-millimeter studies of cold dust and gas in the Magellanic Clouds.” MSc Thesis, University of Chile, Santiago, Chile (2012)
19. Planck collaboration, et al. “Planck early results. XVII. Origin of the submillimetre excess dust emission in the Magellanic Clouds.” *Astron. Astrophys.*, **536**, A17, 17 (2011)
20. Draine, B.T. et al. “Dust masses, PAH abundances, and starlight intensities in the SINGS galaxy sample.” *Astrophys. J.*, **663**, 866–894 (2007)
21. Nikolić, S., Garay, G., Rubio, M., & Johansson, L. E. B. “CO and CS in the Magellanic Clouds: a χ^2 -analysis of multitransitional data based on the MEP radiative transfer model.” *Astron. Astrophys.*, **471**, 561–571 (2007)
22. Dufour, R. J. “The composition of H II regions in the Magellanic Clouds.” IAU Symposium 108, 353–360 (1984)
23. Hunter, D. A., Elmegreen, B. G., & Ludka, B. C. “GALEX ultraviolet imaging of dwarf galaxies and star formation rates.” *Astron. J.*, **139**, 447–475 (2010)

24. Leroy, A.K. et al. “The star formation efficiency in nearby galaxies: measuring where gas forms stars effectively.” *Astron. J.*, **136**, 2782–2845 (2008)
25. Lada, C.J., Forbrich, J., Lombardi, M., & Alves, J.F. “ Star Formation Rates in Molecular Clouds and the Nature of the Extragalactic Scaling Relations.” *Astrophys. J.*, **745**, 190, 6, (2012)
26. Mannucci F. et al., “LSD: Lyman-break galaxies Stellar populations and Dynamics I. Mass, metallicity and gas at $z=3.1$.” *Mon. Not. R. Astron. Soc.*, **398**, 1915-1931 (2009)
27. Engelbracht, C.W. et al. “Metallicity effects on dust properties in starbursting galaxies.” *Astrophys. J.*, **678**, 804–827 (2008)
28. Zhang, H.-X., Hunter, D. A., Elmegreen, B. G., Gao, Y., & Schruba, A. “Outside-in shrinking of the star-forming disks of dwarf irregular galaxies.” *Astron. J.*, **143**, 47, 27 (2012)
29. McMillan, P.J. “Mass models of the Milky Way.” *Mon. Not. R. Astron. Soc.*, **414**, 2446–2457 (2011)
30. Chomiuk, L., Povich, M.S. “Toward a unification of star formation rate determinations in the Milky Way and other galaxies.” *Astron. J.*, **142**, 197, 16 (2011)

Acknowledgements This work was funded in part by the National Science Foundation through grants AST-0707563 and AST-0707426 to DAH and BGE. MR and CV wish to acknowledge support from CONICYT (FONDECYT grant No 1080335). MR was also supported by the Chilean *Center for Astrophysics* FONDAF grant No 15010003. AS was supported by the Deutsche Forschungsgemeinschaft (DFG) Priority Program 1177. We are grateful to Marcus Albrecht for help with the LABOCA data reduction and to Lauren

Hill for making Figure 1a. The National Radio Astronomy Observatory is a facility of the National Science Foundation operated under cooperative agreement by Associated Universities, Inc.

Author Contributions BGE coordinated the observational team, did the calculations for Table 2, and wrote the manuscript; MR did the telescope time justification and with CV observed the galaxy in CO and $870\ \mu\text{m}$ using the APEX telescope with Chilean observing time, reduced the relevant data in Table 1, and also did relevant calculations for Table 2; DH determined the observational strategy, selected WLM for study, chose the observing coordinates, extracted the HI spectra from the LITTLE THINGS data cube, and prepared the figure. EB observed the galaxy on APEX with ESO time and coordinated the work on data uncertainties and background noise. AS made the WLM HI data cube from JVLA observations. All authors discussed the results and commented on the manuscript.

Correspondence and requests for materials should be addressed to bge@us.ibm.com

Table 1: Observations of WLM

Source	Reg.	RA	Dec	Beam (")	Flux
CO(3-2)	A	00:01:57.32	-15:26:49.5	18	$0.200 \pm 0.046 \text{ K km s}^{-1}$
HI	A	00:01:57.32	-15:26:49.5	22	$774 \pm 40 \text{ mJy km s}^{-1}$
870 μm	A	00:01:57.32	-15:26:49.5	22	$2.66 \pm 0.53 \text{ mJy (0.11, 0.02)}^a$
HI	A1	00:01:56.93	-15:26:40.84	45	$4170 \pm 82 \text{ mJy km s}^{-1}$
870 μm	A1	00:01:56.93	-15:26:40.84	45	$15.2 \pm 3.0 \text{ mJy (0.11, 0.06)}^a$
160 μm	A1	00:01:56.93	-15:26:40.84	45	$136.2 \pm 13.6 \text{ mJy (0.05)}^b$
CO(3-2)	B	00:02:1.68	-15:27:52.5	18	$0.129 \pm 0.032 \text{ K km s}^{-1}$

^a Quantities in parentheses are the CO(3-2) flux and the free-free emission, both in mJy, that were subtracted from the source flux before calculating the dust flux. ^b Quantity in parentheses is the free-free emission, in mJy, that was subtracted from the source flux before calculating the dust flux. The average FIR excess factor¹⁸ for the SMC is 1.7, so we divide the CO-corrected and free-free corrected 870 μm fluxes in the table by 1.7 to get the thermal dust flux.

Table 2: Derived Quantities for WLM

Source	Reg.	T , K	Σ , $M_{\odot} \text{ pc}^{-2}$	Mass, M_{\odot}
$\beta = 1.8, \alpha_{\text{CO}} = 124 \pm 60^a$				
Dust	A	14.7 ± 0.7^b	0.053 ± 0.014	$4.6 \pm 1.2 \times 10^2$
Gas ^c	A		$(58 \pm 15)\delta_{\text{GD}}$	$(5.1 \pm 1.3 \times 10^5)\delta_{\text{GD}}$
HI ^d	A		27.3 ± 1.4	$2.4 \pm 0.1 \times 10^5$
H ₂	A		31 ± 15	$1.8 \pm 0.8 \times 10^5$
H ₂ ^e	B		20 ± 10	$1.2 \pm 0.6 \times 10^5$
$\beta = 1.6, \alpha_{\text{CO}} = 34 \pm 34^a$				
Dust	A	15.9 ± 0.8^b	0.032 ± 0.008	$2.8 \pm 0.7 \times 10^2$
Gas ^c	A		$(36 \pm 9)\delta_{\text{GD}}$	$(3.1 \pm 0.8 \times 10^5)\delta_{\text{GD}}$
H ₂	A		8.3 ± 9	$0.5 \pm 0.5 \times 10^5$
H ₂ ^e	B		5.3 ± 6	$0.3 \pm 0.3 \times 10^5$
$\beta = 2, \alpha_{\text{CO}} = 271 \pm 97^a$				
Dust	A	13.6 ± 0.6^b	0.087 ± 0.022	$7.5 \pm 1.9 \times 10^2$
Gas ^c	A		$(95 \pm 24)\delta_{\text{GD}}$	$(8.3 \pm 2.1 \times 10^5)\delta_{\text{GD}}$
H ₂	A		67 ± 24	$3.9 \pm 1.4 \times 10^5$
H ₂ ^e	B		44 ± 16	$2.5 \pm 0.9 \times 10^5$

Table 2 notes: ^a The units of α_{CO} are $M_{\odot} \text{ pc}^{-2} (\text{K km s}^{-1})^{-1}$; the uncertainty is dominated by the uncertainties in the 160 μm and 870 μm fluxes, as indicated by their error limits in Table 1; the error limits are approximately symmetric. ^b The dust temperature in region A is assumed to be the same as the measured dust temperature in region A1. ^c $\delta_{\text{GD}} = R_{\text{GD}}/1100$ is the gas to dust ratio R_{GD} normalized to that of the Milky Way scaled to the metallicity of WLM. Lowering δ_{GD} lowers α_{CO} , but this does not seem reasonable: Engelbracht et al.²⁷ show a correlation suggesting $M_{\text{gas}}/M_{\text{dust}} \sim 5000$ when $12 + \log(\text{O}/\text{H}) = 7.8$, and this implies larger $\delta_{\text{GD}} \sim 4.5$ and α_{CO} . The gas mass and resulting α_{CO} also depend on the assumed correction factor of 1.7 for sub-mm excess. With no sub-mm excess correction, α_{CO} increases for all β : at $\beta = 1.8$, $\alpha_{\text{CO}} = 370$. Solutions with no sub-mm excess correction and lower β ¹⁹ are in the Supplementary material. In addition, α_{CO} depends on the assumed ratio CO(3-2)/CO(1-0), which was taken to be 0.8 for the table; a value of CO(3-2)/CO(1-0)= 1 increases α_{CO} to 155 for $\beta = 1.8$. ^d The HI mass column density is corrected for He and heavy elements. ^e The molecular mass for region B was calculated using the CO integrated intensity and the value of α_{CO} determined from Region A.

Table 3: (Alternate Method) Derived Quantities for WLM with no sub-mm Excess Correction

Source	Reg.	T , K	Σ , $M_{\odot} \text{ pc}^{-2}$	Mass, M_{\odot}
$\beta = 1.2, \alpha_{\text{CO}} = 0.6 \pm 17$				
Dust	A	16.5 ± 0.9	0.025 ± 0.007	$2.2 \pm 0.6 \times 10^2$
Gas	A		$(27 \pm 7)\delta_{\text{GD}}$	$(2.4 \pm 0.6 \times 10^5)\delta_{\text{GD}}$
HI	A		27.3 ± 1.4	$2.4 \pm 0.1 \times 10^5$
H ₂	A		0.15 ± 7	$0.09 \pm 4.2 \times 10^4$
H ₂	B		0.1 ± 4.7	$0.06 \pm 2.6 \times 10^4$
$\beta = 1.4, \alpha_{\text{CO}} = 72 \pm 47$				
Dust	A	15.2 ± 0.7	0.041 ± 0.011	$3.6 \pm 0.9 \times 10^2$
Gas	A		$(45 \pm 12)\delta_{\text{GD}}$	$(3.9 \pm 1.0 \times 10^5)\delta_{\text{GD}}$
H ₂	A		18 ± 12	$1.0 \pm 0.7 \times 10^5$
H ₂	B		11.6 ± 7.5	$6.7 \pm 4.4 \times 10^4$
$\beta = 1.6, \alpha_{\text{CO}} = 186 \pm 75$				
Dust	A	14.1 ± 0.6	0.067 ± 0.017	$5.8 \pm 1.5 \times 10^2$
Gas	A		$(74 \pm 19)\delta_{\text{GD}}$	$(6.4 \pm 1.6 \times 10^5)\delta_{\text{GD}}$
H ₂	A		46 ± 19	$2.7 \pm 1.1 \times 10^5$
H ₂	B		30 ± 12	$1.7 \pm 0.7 \times 10^5$

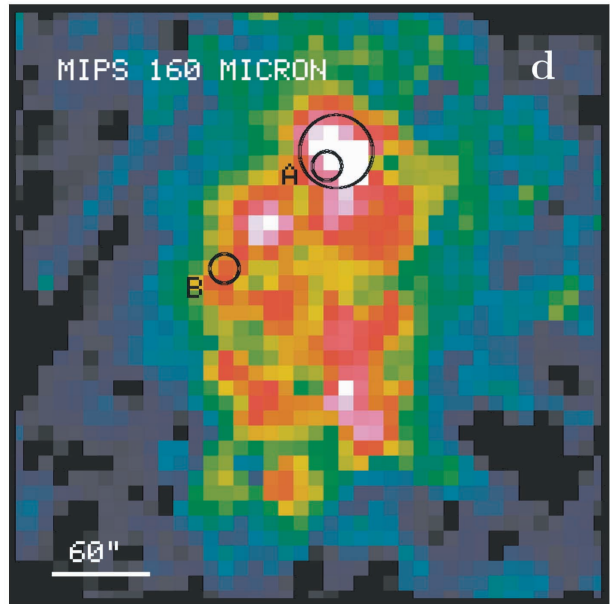
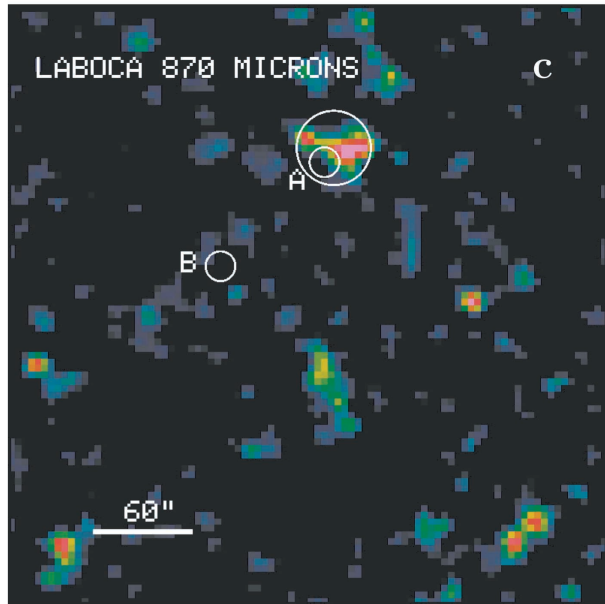
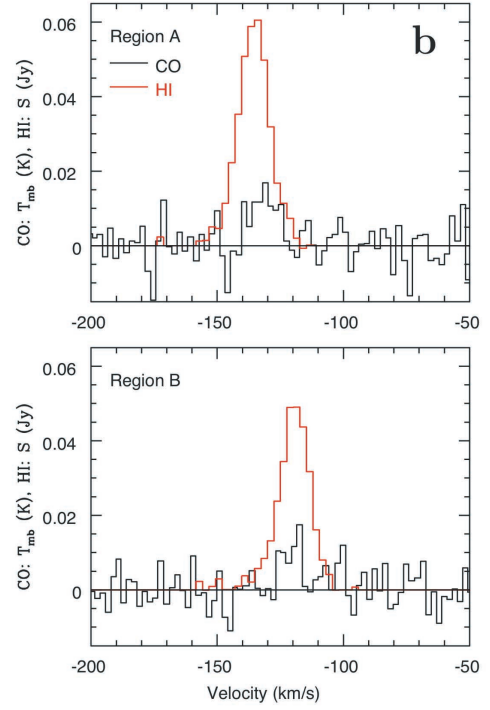
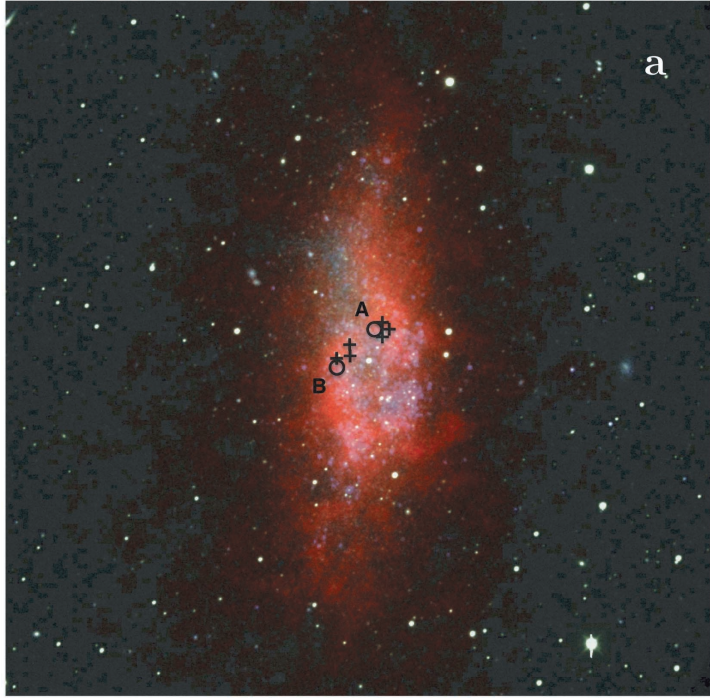


Figure 1 WLM is a small, gas-rich galaxy 985 ± 33 kpc from the Milky Way⁴. It contains $1.6 \times 10^7 M_{\odot}$ of stars²⁸, compared to $6.4 \pm 0.6 \times 10^{10} M_{\odot}$ in the Milky Way²⁹, and it forms new stars at a rate²³ of $0.006 M_{\odot} \text{ yr}^{-1}$, which is 12 times higher per unit stellar mass than the Milky Way³⁰. In the top-left color composite, red is HI, green is V-band and blue is GALEX FUV. The HI has $7.6''$ and 2.6 km s^{-1} resolution, and the CO(3-2) has $18''$ (circles) and 0.11 km s^{-1} resolution, although the CO(3-2) spectra shown in the figure were smoothed to 2.2 km s^{-1} resolution. The CO detections are labeled; their exposure times were 218 (Region A) and 248 (Region B) minutes. Other searched regions with factors of ~ 2 to ~ 6 shorter exposure times are shown by plus marks; the presence of comparable CO in some of these other regions cannot be ruled out. Upper right: Spectra of the two detections: velocities are Local Standard of Rest; CO is main beam brightness temperature T_{mb} in units of Kelvin; HI is flux in units of Jy. Lower left: False color image of the $870 \mu\text{m}$ observations taken with LABOCA on APEX. Lower right: False color *Spitzer* $160 \mu\text{m}$ image obtained from *Spitzer* archives. The $870 \mu\text{m}$ and $160 \mu\text{m}$ images display the same field of view. In the lower panels, the small circles show where CO was detected and are displayed with $22''$ diameter, which is the resolution of LABOCA. The large circle is $45''$ in diameter and surrounds a large HI and FIR cloud (A1) where the dust temperature was measured.